PAPER

Carbon tips for all-carbon single-molecule electronics

Y. J. Dappe,*[a] C. González[b] and J. C. Cuevas[c]

We present here an exhaustive *ab initio* study of the use of carbon-based tips as electrodes in single-molecule junctions. Motivated by recent experiments, we show that carbon tips can be combined with other carbon nanostructures, such as graphene, to form all-carbon molecular junctions with molecules like benzene or C_{60}. Our results show that the use of carbon tips can lead to relatively conductive molecular junctions. However, contrary to junctions formed with standard metals, the conductance traces recorded during the formation of the all-carbon single-molecule junctions do not exhibit clear conductance plateaus, which can be attributed to the inability of the hydrogenated carbon tips to form chemical bonds with the organic molecules. Additionally, we explore here the use of carbon tips for scanning tunneling microscopy and show that they are well suited for obtaining sample images with atomic resolution.

Introduction

One of the central goals of molecular electronics is the understanding of the electron transport through single molecules.[1] Basic prerequisites to achieve this goal are the ability to fabricate very reliable single-molecule junctions and the possibility of exploring a wide range of molecules. So far, the fabrication of most molecular junctions has been based on the use of electrodes made of conventional metals, which limits somehow the type of molecules to be investigated. In particular, gold has been frequently the material of choice for the electrodes because of its chemical inertness and the fact that molecules can be bound to it by means of standard anchoring groups such as thiol,[2–4] amine,[5] nitro,[6] nitrile,[7] or even fullerene.[8] Other more reactive metals, as for instance Pt[9,10] and Ag,[11] have also been used as electrode materials. In the search for new and more versatile metal–molecule combinations, it is natural to think of carbon-based electrodes as a likely step towards all-carbon single-molecule electronics. An important breakthrough in this direction was achieved by Nuckolls and coworkers[12–14] who demonstrated that single-walled carbon nanotubes (SWNTs) can be used as electrodes in single-molecule junctions. Although this approach has opened fascinating possibilities, it also has some disadvantages such as the inability to control the metal–molecule distance *in situ*. An alternative to the SWNTs has been recently provided by Castellanos-Gomez *et al.*[15] who have shown that carbon fiber tips can be used to form single-molecule junctions in the spirit of STM-based break junctions. In particular, these authors have applied the carbon fiber tips in molecular junctions with monothiolated alkane chains, something that is not easy to realize using gold electrodes. This experimental work naturally raises a number of fundamental questions such as: what is the nature of the carbon tip–molecule bonding?, what are the signatures of the junction formation in the case of carbon electrodes?, can the use of carbon tips lead to more conductive molecular junctions?, or can these tips be combined with other carbon-based structures, such as graphene, to form all-carbon single-molecule junctions?

The goal of this work is to address these basic questions and for this purpose, we present here a thorough *ab initio* study of the electronic transport of single-molecule junctions based on the use of carbon fiber tips. In particular, we show that carbon tips can be combined with a graphene electrode to form junctions with single benzene and C_{60} molecules, which are ideal examples of all-carbon-based single-molecule junctions. Additionally, and as a bonus of our study, we have found that carbon fiber tips can be used as excellent STM tips, leading to atomic resolution images as obtained with standard metallic tips.

Theory

The first step in our theoretical study is the modeling of the carbon tips and their electrical characterization. The tip used throughout this work is shown in Fig. 1a. This tip has been modeled as three pieces of stacked hydrogenated graphene sheets, exhibiting a single hydrogen-decorated carbon atom at one extremity, which improves the atomic resolution in STM image calculations as previously reported.[16]

[a]*Service de Physique de l'Etat Condensé (CNRS URA2464), IRAMIS, CEA Saclay, 91191 Gif-Sur-Yvette, France. E-mail: yannick.dappe@cea.fr*

[b]*Departamento de Física, Universidad de Oviedo, 33006 Oviedo, Spain*

[c]*Departamento de Física Teórica de la Materia Condensada and Condensed Matter Physics Center (IFIMAC), Universidad Autónoma de Madrid, 28049 Madrid, Spain*
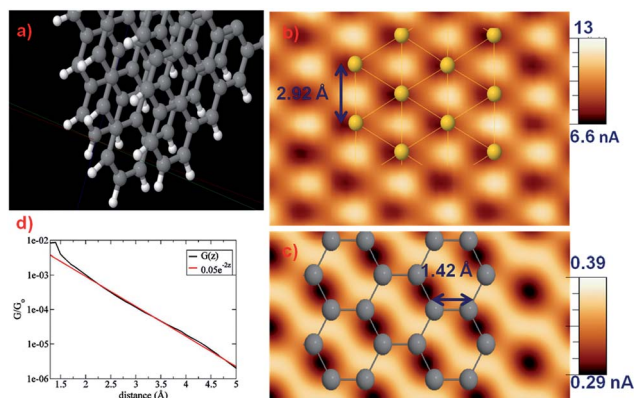
Fig. 1 (a) Geometric model for the hydrogen decorated graphitic tip. The tip is formed by three triangular graphene sheets, stacked together through van der Waals interactions at an equilibrium distance of 3.1 Å. (b) Computed STM image of the Au(111) surface. The tip–sample distance was fixed at 4 Å and the bias voltage was 0.1 V. The gold surface atoms are superimposed. (c) Computed STM image of a graphene plane under the same conditions as in (b). The corresponding structure has also been superimposed. (d) Conductance (black line) in units of G_0 on a logarithmic scale *versus* vertical tip displacement above the graphene plane. The red curve corresponds to a fit to an exponential function, as indicated in the legend.

The presence of hydrogen atoms ensures the stability of the graphitic tip reducing its reactivity with possible contamination. The H atoms were introduced here to mimic the experimental conditions of the work of Castellanos-Gomez *et al.*[15] The electronic structure of this tip, and of all the systems studied in this work, was described using a very efficient density functional theory (DFT) molecular dynamics technique (FIREBALL).[17,18] The FIREBALL package uses a localized optimized minimal basis set,[19] and the self-consistency is achieved over the occupation numbers through the Harris functional.[20] Besides, the LDA exchange-correlation energy is calculated using the efficient multi-center weighted exchange-correlation density approximation (McWEDA).[21,22]

It is worth stressing that equilibrium configurations of the molecular junctions were determined taking into account the van der Waals (vdW) forces. This was done making use of the LCAO-S^2 + vdW formalism.[23–27] This approach is based on the balance between two contributions. The first one, due to the small overlaps between electronic densities of the two interacting subsystems, yields a repulsive interaction. Therefore, this energy, that we call "weak chemical interaction", can be determined as an expansion of the wave-functions and operators with respect to these overlaps. The second contribution, which corresponds to the pure van der Waals interaction, is based on a dipole–dipole interaction between the subsystems. Both contributions are added within a perturbation theory to the total energy of the system. More details have been given elsewhere.[23]

Results and discussion

STM images using carbon based tips

To characterize the electrical behavior of this graphitic electrode, we have investigated its use as a tip in scanning tunneling

microscopy. Indeed, different experimental groups have reported atomic resolution STM images recorded with carbon-based tips,[28–30] and, in particular, with carbon fiber tips.[31] To confirm that our tip is not only metallic, but it can also produce high resolution topographic maps of a surface, we have first investigated the STM images of a Au(111) surface. The gold surface has been modeled using a 4×4 supercell in the xy plane of four layers and a single k-point, while the STM images were calculated using a well-established non-equilibrium Keldysh–Green formalism which takes multiple scattering into account.[32,33] The images were processed with the WSxM software from Nanotec.[34] As shown in Fig. 1b, our carbon tip provides indeed a STM image of the gold surface with atomic resolution.

To further characterize our carbon tip, we have also investigated the STM image of a graphene plane, as represented in Fig. 1c. Here also the carbon tip provides an image with atomic resolution. This image compares well with experimental studies of graphene STM imaging using a metallic tip.[35] Apparently, an important difference is found when the theoretical currents are compared with the experimental values presented in ref. 31. However, moving down the tip to 1 Å, the resulting maximum/minimum current increases to 12/5 nA in better agreement with the measurements. In our calculations, the tip–graphene distance is referred to the last hydrogen atom of the tip, with the carbon atoms participating in the tunnelling process placed 1.9 Å higher. This justifies the tip approach in order to improve the resolution. Moreover, the low interaction of the tip with the substrate allows the approach to maintain the integrity of the tip. In both images, Au(111) and graphene, although each maximum corresponds to one atom, the bright protrusions appear displaced from the atomic positions. In the case of graphene, as is well-known, only the p_z orbital of the C-atoms has a contribution in the density of states but several atoms can interact with the dominating p_y-orbitals of the C-atoms in the graphitic tip. As a result, the higher current is obtained when the tip is placed at some points between the C-atoms instead of over them. In the Au image, this effect is added to the complex interactions with different kinds of orbitals of each Au atom.

Additionally, we have studied the transition between the tunneling and the contact regime as the carbon tip approaches the graphene plane. This crossover is shown in Fig. 1d where the linear conductance is presented as a function of the tip–sample distance (d). The transition to the contact regime at short distances is signalized by the presence of a saturation of the conductance that reaches a value of around $0.01G_0$, where $G_0 = 2e^2/h$ is the quantum of conductance. In the tunneling regime, the conductance decreases exponentially with the tip–surface distance as $G \propto \exp(-\beta d)$, where $\beta = 2.0$ Å^{-1}. This exponent is slightly larger than, for instance, the theoretical exponent found in the breaking of the gold atomic-size contact.[36]

The results discussed above clearly suggest that carbon tips can lead to atomic resolution in STM imaging with a quality comparable to that of standard metallic tips. To further confirm this impression, we have also simulated the imaging of simple organic molecules. In Fig. 2 we compare the STM images obtained with the carbon and copper tips of a single benzene molecule physisorbed on a graphene plane.
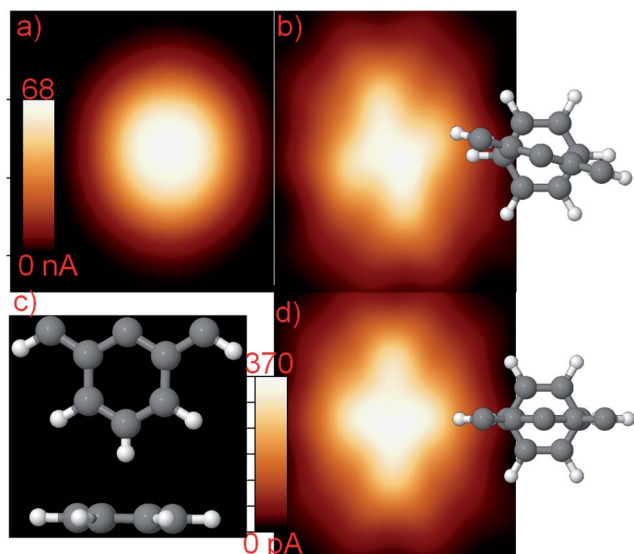
Fig. 2 Comparison of STM image calculations of benzene on graphene using (a) the Cu tip and (b and d) the graphitic tip for two orientations. The corresponding geometries of the benzene molecule with the graphitic tip are presented on the right side. In (c) a lateral view of the tip falling over the center of the hexagon is shown. All the calculations were performed using a voltage of 0.1 V and a tip–benzene distance of 4 Å.

The equilibrium position of the benzene molecule 3.1 Å above the graphene sheet was determined taking into account the van der Waals (vdW) forces. As one can see in Fig. 2, the carbon tip provides a different image (b and d) compared to the copper tip (a), breaking the circular symmetry of the bright spot. Although the maximum is still placed in the centre of the hexagon, four arms appear producing a kind of cross-shape structure when the carbon tip is used. This new structure is influenced by the tip orientation with respect to the molecule as can be observed by comparing Fig. 2b and d. The orientation of the four arms in Fig. 2b suggests how the hexagon structure could be formed in graphene where successive hexagons are joined. In fact, the inclusion of the C atoms around produces a split in the maximum at the centre of the hexagon ring resulting in an atomic-like resolution in the graphene sheet (not clearly observed in Fig. 1).

Furthermore, the weak interaction with the substrates makes this tip less invasive. From an experimental point of view, the carbon tip presents important advantages, due to the flexibility and the functionalization ability of the tip. Thus, for instance, in contact mode STM or AFM, this tip would allow us to reproduce the results reported by Gross et al.[37] who used (CO)-functionalized metallic tips.

All-carbon single-molecule junctions

We turn now to the central issue of this work, namely the formation of single-molecule junctions with carbon tips. The first example that we analyze here is the carbon tip–benzene–graphene junction discussed in the previous paragraph. Now, we explore the conductance of this junction when the carbon tip

approaches the benzene molecule to reach the contact regime. The summary of our main results can be seen in Fig. 3. First of all, in the left panels (a–c) we show the junction geometry for three characteristic distances, from the tunneling regime in panel (a) to the contact one in panel (c). This distance corresponds to the separation between the apical hydrogen atom on the tip and the nearest carbon atom of the molecule. Let us stress that to simulate the junction formation, we have made the tip approach in a step-wise manner, with steps of 0.5 Å at small distances and of 1 Å at longer distances, and after every step, we have performed a DFT geometry relaxation of the whole junction until the forces became lower than 0.1 eV Å^{-1}. Notice that there is no sign of a chemical bond at any step between the tip and the molecule. In the short-distance regime, see Fig. 3c, the tip is deformed while the molecule is shifted. In other words, the tip–molecule interaction seems to be dominated by vdW forces all the way to the contact regime. For every relaxed structure the conductance was evaluated using the methodology mentioned above.[32]

In Fig. 3d we show the corresponding results of the transmission as a function of energy for different tip–molecule distances. Let us remind that in the spirit of the Landauer formalism, the linear conductance at low temperature is determined by the transmission coefficient at the Fermi energy (E_F) as $G = G_0 T(E_F)$. As one can see, the transmission around the Fermi energy is dominated by a double resonance, which can be associated with the highest occupied molecular orbital (HOMO) and with the lowest unoccupied molecular orbital (LUMO) of the benzene molecule. These frontier orbitals are separated in our DFT approach by 5.6 eV in the junctions, which is a bit smaller than the value in the gas phase (6.13 eV) due to the weak
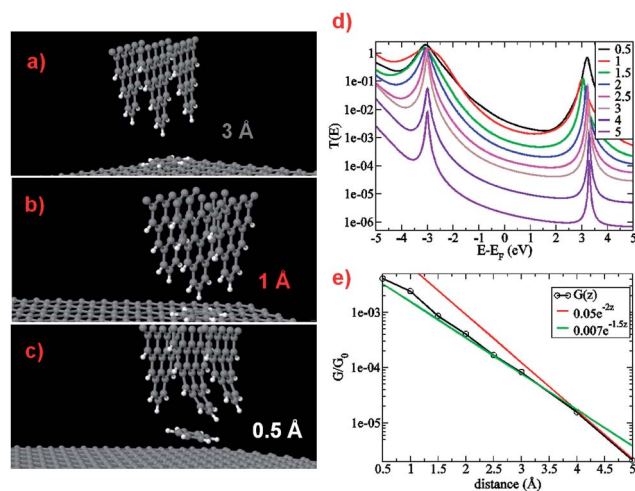

Fig. 3 Geometric representation of the graphene tip in interaction with a benzene molecule adsorbed on graphene (a) at a long distance, (b) at an intermediate distance, and (c) in the short distance regime (notice the deformation of the tip). (d) Transmission as a function of energy on a logarithmic scale for benzene on graphene using the graphene tip, at different vertical distances (in Å). (e) Conductance as a function of the tip–molecule distance on a logarithmic scale (black line). The red and green lines correspond to exponential fits in different distance regions (the functions are indicated in the legend).

interaction with the graphene plane. The Fermi energy lies close to the middle of the HOMO–LUMO gap, only slightly closer to the HOMO. The corresponding linear conductance is shown in Fig. 3e and as it can be observed, it varies exponentially from the tunneling regime (red line in Fig. 3e) to the contact one (green line). When the tip–molecule distance becomes really small and the tip starts to be deformed, the conductance reaches a maximum value of $0.004 G_0$. This maximum value is due to the increasing number of tunneling atoms during the tip approach. On the other hand, in the case of metallic tips, the conductance increases in the short-distance regime due to the formation of chemical bonds, leading to a saturation of the conductance. Although this value is clearly lower than the maximum of around $1 G_0$ found for a benzene junction with Pt electrodes,[10] due to the stronger Pt–benzene interaction, it is still comparable to other metal–molecule–metal junctions[1] despite the reduced density of states of graphene at the Fermi level as compared to metallic electrodes. More importantly, the conductance–distance curve does not exhibit any clear plateau, which is the usual signature of the formation of molecular junctions.[38] Such a plateau is usually attributed to the formation of a strong bond, usually covalent, which makes the conductance relatively insensitive to the variation of the metal–molecule distance within a certain range. The absence of this feature in our case is consistent with the lack of formation of a chemical bond, as is evident in Fig. 3c. However, as it is apparent from the two different fits shown in Fig. 3e, the attenuation factor β varies with distance. This behavior is due to the progressive deformation of the tip induced by the repulsive interaction with the molecule, which modulates the exponential decay of the conductance. Notice finally that at long distances we recover the typical conductance behavior of the graphene–tip interaction as discussed earlier. So in short, this first analysis suggests that while a carbon-tip-based molecular junction may exhibit a relatively high conductance, the actual value depends very sensitively on the tip–molecule distance because of the inability to form a true chemical bond.

Let us mention that since our results are based on standard DFT methods, it is likely that we are overestimating the conductance of the molecular junctions as a consequence of the known underestimation of the HOMO–LUMO gap.[1] These deficiencies are known to be due to exchange and correlation effects that are not properly described with conventional exchange–correlation functionals.

The next example that we want to discuss here is an all-carbon single-molecule junction where a C_{60} molecule physisorbed on a graphene sheet is contacted by the carbon tip, see Fig. 4.

In order to construct this junction, we have first calculated the equilibrium distance between the C_{60} molecule and the graphene plane. Again, using the LCAO-S^2 + vdW formalism[23] to describe the dispersion forces, we have found an equilibrium distance of 2.9 Å for an adsorption energy of 1 eV, in good agreement with previous calculations.[24] Then, to simulate the junction formation, we have followed the same procedure as in the previous case of benzene on graphene. Fig. 4a–c show three different snapshots of the formation of the junction. As in the
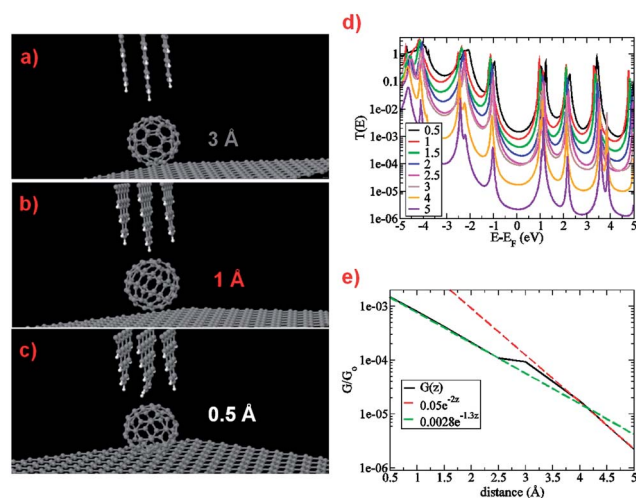

Fig. 4 Geometric representation of the graphene tip interacting with a C_{60} molecule adsorbed on graphene (a) at a long distance, (b) at an intermediate regime and (c) the short distance (see again the deformation of the tip). (d) Transmission as a function of energy on a logarithmic scale for C_{60} on graphene using the carbon tip, at different vertical distances. (e) Linear conductance in units of G_0 on a logarithmic scale for C_{60} on graphene using the graphene tip, at different vertical distances. Three different fits are also represented to stress the three different conductance regimes.

case of the benzene molecule, the carbon tip did not bond with the molecule at any step and it is deformed when it is brought close to the C_{60}, which means that the tip–molecule interaction is not sufficiently strong to modify the hybridization of the carbon atoms of either the tip or the molecule. This is in marked contrast to what happens in the case of a junction with a Cu tip. In ref. 33, the same procedure was applied to the description of a contact-STM experiment, where a Cu tip interacted with a C_{60} molecule adsorbed over a metallic surface. In that case, a strong hybridization of the tip with the C_{60} was observed, as illustrated in Fig. 5.

As a consequence of this hybridization, a plateau was found in the conductance trace and also an enlarged STM image in the contact zone. In the case of the carbon tip, the hydrogen saturation of the tip hinders the hybridization between the tip and the molecule, leading to a strong deformation of the tip to avoid the bonding. Turning to the transmission characteristics, as we show in Fig. 4d, the low-bias transport is dominated almost equally by the HOMO and LUMO (notice that the Fermi energy lies more or less in the middle of the gap). The HOMO–LUMO gap of 2.00 eV observed in the transmission curves agrees well with the value found in the gas phase (2.17 eV) within our DFT approach, which is another indication of the relatively weak tip–molecule interaction at all distances.

In Fig. 4e, we show the evolution of the conductance, on a logarithmic scale, as a function of the tip–molecule distance. The conductance reaches a maximum value of $0.0015\ G_0$, which is in the same range as the result for the benzene junction. However, this value is clearly lower than the corresponding one when the molecule is sandwiched by metallic tips and surfaces.[33,40] Moreover, we can observe three different regimes,
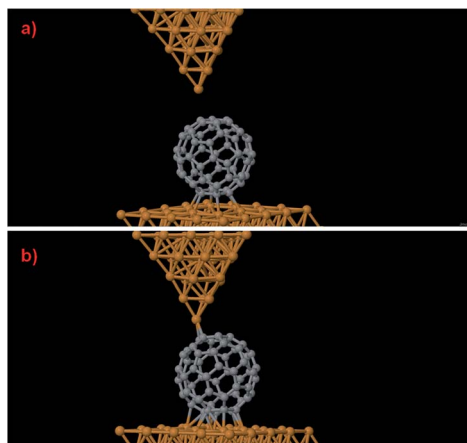
Fig. 5 Calculated geometries of a Cu–tip–C_{60} junction calculated for different positions: (a) far distance and (b) contact mode. One can observe the formation of a molecular contact between the tip and the molecule, in contrast to the situation with the carbon tip.

as stressed by the fits in the different zones. First, we recover at a long distance the conductance behavior of the graphene conductance, as it was the case previously for benzene. Second, we reach a short plateau with a small attenuation factor of $\beta = 0.25$ Å^{-1}. In this situation, the tip–molecule distance is maintained constant due to the small deformation of the C_{60} in repulsive interaction with the tip. Third, the conductance increases again, now with $\beta = 1.3$ Å^{-1}, when the tip is deformed and consequently is able to come closer to the molecule, without however forming a bond. This explains the absence of a
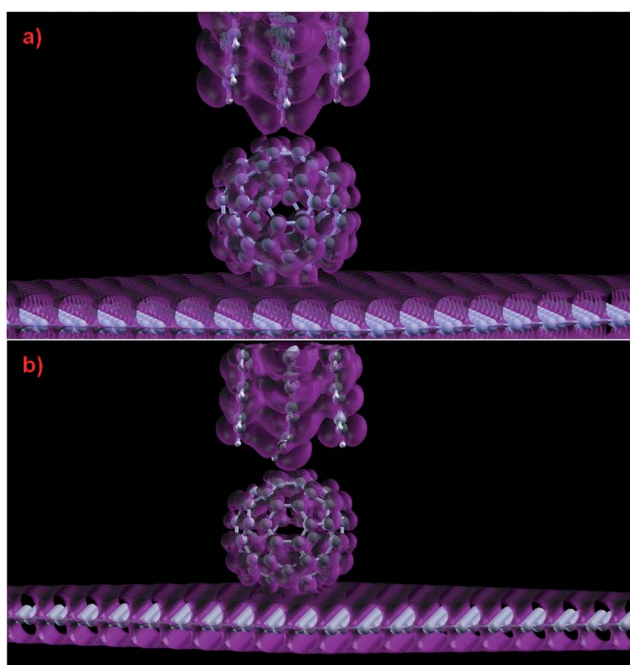

Fig. 6 Isosurface plots of the density of states at the Fermi energy, showing the carbon tip–C_{60} contact at (a) 1.5 Å and (b) 0.5 Å where the tip is highly deformed and no strong bonding to the C_{60} is predicted.

clear plateau in the contact regime. This behavior is further illustrated in Fig. 6 where we have represented the isosurface of the density of states at the Fermi energy of the molecular junction for two tip–C_{60} distances: (a) at 1.5 Å and (b) at 0.5 Å. In both cases we can observe that there is almost no hybridization of the electronic densities, which confirms the fact that the carbon tip does not bond with the molecule.

It is worth commenting the connection between our results and the experiments of Castellanos-Gomez[15,39] where molecular junctions were formed between carbon tips and octanethiol self-assembled monolayers. In those experiments, the appearance of rather short plateaus was reported, which was tentatively attributed to the formation of a chemical bond between the tip and the non-thiolated end of the molecule. Our simulations of the C_{60}-junctions show that short plateaus may appear as a result of the tip deformation, while the interaction is still of van der Waals type. Thus, it is not obvious that one can exclude the mechanical origin of the observed plateaus in ref. 15 and 39. This is an issue that we will address in detail in a forthcoming publication.

Conclusions

In summary, we have presented the first full theoretical characterization of a carbon tip used as an electrode in a single-molecule junction. In particular, we have combined this tip with graphene as a counter electrode, and benzene or C_{60} molecule to build molecular junctions. We have demonstrated that this new type of junction is relatively conductive, but presents different behaviors compared to metal–organic junctions. More specifically, we have observed that the carbon tip–molecule junction is not strongly bonded, the interaction being ruled by van der Waals forces. Consequently, there is no real contact regime in this kind of junction, as we do not observe a conductance plateau as is the case when using metallic electrodes. Furthermore, we have shown that this new tip can also be used for STM characterization, yielding atomic resolution similar to what is observed with a metallic tip. Our results provide a clear route towards an all-carbon molecular electronics, and future work will focus on designing new molecular electronic devices based on these tips. Extended analysis of STM imaging using this new tip will also be explored raising many perspectives in STM/AFM imaging with non-invasive tips.

Conflict of interest

The authors declare no competing financial interest.

Acknowledgements

Notes and references

1 J. C. Cuevas and E. Scheer, *Molecular Electronics: An Introduction to Theory and Experiment*, World Scientific, Singapore, 2010.

2 M. A. Reed, C. Zhou, C. J. Muller, T. P. Burgin and J. M. Tour, *Science*, 1997, **278**, 252.

3 X. Li, J. He, J. Hihath, B. Xu, S. M. Lindsay and N. J. Tao, *J. Am. Chem. Soc.*, 2006, **128**, 2135.

4 C. Li, I. Pobelov, T. Wandlowski, A. Bagrets, A. Arnold and F. Evers, *J. Am. Chem. Soc.*, 2008, **130**, 318.

5 L. Venkataraman, J. E. Klare, I. W. Tam, C. Nuckolls, M. S. Hybertsen and M. L. Steigerwald, *Nano Lett.*, 2006, **6**, 458.

6 L. A. Zotti, T. Kirchner, J. C. Cuevas, F. Pauly, T. Huhn, E. Scheer and A Erbe, *Small*, 2010, **6**, 1529–1535.

7 A. Mishchenko, L. A. Zotti, D. Vonlanthen, M. Bürkle, F. Pauly, J. C. Cuevas, M. Mayor and T. Wandlowski, *J. Am. Chem. Soc.*, 2011, **133**, 184.

8 C. A. Martin, D. Ding, J. K. Sørensen, T. Bjørnholm, J. M. van Ruitenbeek and H. S. J. van der Zant, *J. Am. Chem. Soc.*, 2008, **130**, 13198.

9 R. H. M. Smit, Y. Noat, C. Untiedt, N. D. Lang, M. C. van Hemert and J. M. van Ruitenbeek, *Nature*, 2002, **419**, 906.

10 M. Kiguchi, O. Tal, S. Wohlthat, F. Pauly, M. Krieger, D. Djukic, J. C. Cuevas and J. M. van Ruitenbeek, *Phys. Rev. Lett.*, 2008, **101**, 46801.

11 T. Kim, H. Vázquez, M. S. Hybertsen and L. Venkataraman, *Nano Lett.*, 2013, **13**, 3358–3364.

12 X. Guo, J. P. Small, J. E. Klare, Y. Wang, M. S. Purewal, I. W. Tam, B. H. Hong, R. Caldwell, L. Huang, S. O'Brien, J. Yan, R. Breslow, S. J. Wind, J. Hone, P. Kim and C. Nuckolls, *Science*, 2006, **311**, 356–359.

13 X. Guo and C. Nuckolls, *Acc. Chem. Res.*, 2008, **41**, 1731–1741.

14 X. Guo, A. A. Gorodetsky, J. Hone, J. K. Barton and C. Nuckolls, *Nat. Nanotechnol.*, 2008, **3**, 163–167.

15 A. Castellanos-Gomez, S. Bilan, L. A. Zotti, C. R. Arroyo, N. Agraït, J. C. Cuevas and G. Rubio-Bollinger, *Appl. Phys. Lett.*, 2011, **99**, 123105.

16 J. I. Martínez, E. Abad, C. González, F. Flores and J. Ortega, *Phys. Rev. Lett.*, 2012, **108**, 246102.

17 J. P. Lewis, *et al.*, *Phys. Rev. B: Condens. Matter Mater. Phys.*, 2001, **64**, 195103.

18 P. Jelínek, H. Wang, J. P. Lewis, O. F. Sankey and J. Ortega, *Phys. Rev. B: Condens. Matter Mater. Phys.*, 2005, **71**, 235101.

19 O. F. Sankey and D. J. Niklewski, *Phys. Rev. B: Condens. Matter Mater. Phys.*, 1989, **40**, 3979–3995.

20 J. P. Lewis, *et al.*, *Phys. Status Solidi B*, 2011, **248**, 1989–2007.

21 M. A. Basanta, Y. J. Dappe, P. Jelínek and J. Ortega, *Comput. Mater. Sci.*, 2007, **39**, 759.

22 A. A. Demkov, J. Ortega, O. F. Sankey and M. P. Grumbach, *Phys. Rev. B: Condens. Matter Mater. Phys.*, 1995, **52**, 1618.

23 Y. J. Dappe, M. A. Basanta, J. Ortega and F. Flores, *Phys. Rev. B: Condens. Matter Mater. Phys.*, 2006, **74**, 205434.

24 Y. J. Dappe, J. Ortega and F. Flores, *Phys. Rev. B: Condens. Matter Mater. Phys.*, 2009, **79**, 165409.

25 M. Seydou, Y. J. Dappe, S. Marsaudon, J. P. Aime, X. Bouju and A. M. Bonnot, *Phys. Rev. B: Condens. Matter Mater. Phys.*, 2011, **83**, 045410.

26 M. Švec, P. Merino, Y. J. Dappe, C. González, E. Abad, P. Jelínek and J. A. Martín-Gago, *Phys. Rev. B: Condens. Matter Mater. Phys.*, 2012, **86**, 121407(R).

27 Y. J. Dappe and J. I. Martinez, *Carbon*, 2013, **54**, 113.

28 T. Ohmori, L. A. Nagahara, K. Hashimoto and A. Fujishima, *Rev. Sci. Instrum.*, 1994, **65**, 404–406.

29 R. Colton, S. Baker, J. Baldeschwieler and W. Kaiser, *Phys. Lett.*, 1987, **51**, 305.

30 D. Rohlfing and A. Kuhn, *Electroanalysis*, 2007, **19**, 121–128.

31 A. Castellanos-Gomez, N. Agraït and G. Rubio-Bollinger, *Nanotechnology*, 2010, **21**, 145702.

32 J. M. Blanco, *et al.*, *Phys. Rev. B: Condens. Matter Mater. Phys.*, 2004, **70**, 085405.

33 G. Schull, Y. J. Dappe, C. González, H. Bulou and R. Berndt, *Nano Lett.*, 2011, **11**, 3142.

34 I. Horcas, R. Fernández, J. M. Gómez-Rodriguez, J. Colchero, J. Gómez-Herrero and A. M. Baro, *Rev. Sci. Instrum.*, 2007, **78**, 013705.

35 A. L. Vázquez de Parga, F. Calleja, B. Borca, M. C. G. Passeggi, Jr, J. J. Hinarejos, F. Guinea and R. Miranda, *Phys. Rev. Lett.*, 2008, **100**, 056807.

36 D. R. Ward, F. Hüser, F. Pauly, J. C. Cuevas and D. Natelson, *Nat. Nanotechnol.*, 2010, **5**, 732.

37 L. Gross, F. Mohn, N. Moll, B. Schuler, A. Criado, E. Guitián, D. Peña, A. Gourdon and G. Meyer, *Science*, 2012, **337**, 1326.

38 B. Xu and N. J. Tao, *Science*, 2003, **301**, 1221.

39 G. Rubio-Bollinger, A. Castellanos-Gomez, S. Bilan, L. A. Zotti, C. R. Arroyo, N. Agraït and J. C. Cuevas, *Nanoscale Res. Lett.*, 2012, **7**, 254.

40 N. Néel, J. Kröger, L. Limot, T. Frederiksen, M. Brandbyge and R. Berndt, *Phys. Rev. Lett.*, 2007, **98**, 065502.